Biochimica et Biophysica Acta 1848 (2015) 544–553

Contents lists available at ScienceDirect

Biochimica et Biophysica Acta

journal homepage: www.elsevier.com/locate/bbamem

Novel endosomolytic peptides for enhancing gene delivery in nanoparticles

Aqeel Ahmad [a,1], Sanjeev Ranjan [a,1,2], Weikai Zhang [b], Jing Zou [b], Ilmari Pyykkö [b], Paavo K.J. Kinnunen [a,*]

[a] Helsinki Biophysics and Biomembrane Group, Department of Biomedical Engineering and Computational Science, Aalto University School of Science, Espoo, Finland
[b] Department of Otolaryngology, University of Tampere, Medical School, Tampere, Finland

ARTICLE INFO

Article history:
Received 21 March 2014
Received in revised form 28 October 2014
Accepted 6 November 2014
Available online 15 November 2014

Keywords:
Endosomolytic peptides
Endosomal escape
Nanoparticles
Gene delivery
Transfection
Gene expression

ABSTRACT

Trapping in the endosomes is currently believed to represent the main barrier for transfection. Peptides, which allow endosomal escape have been demonstrated to overcome this barrier, similarly to the entry of viruses. However, the design principles of such endosomolytic peptides remain unclear. We characterized three analogs derived from membrane disrupting antimicrobial peptides (AMP), viz. LL-37, melittin, and bombolitin V, with glutamic acid substituting for all basic residues. These analogs are pH-sensitive and cause negligible membrane permeabilization and insignificant cytotoxicity at pH 7.4. However, at pH 5.0, prevailing in endosomes, membrane binding and hemolysis of human erythrocytes become evident. We first condensed the emerald green fluorescent protein (emGFP) containing plasmid by protamine, yielding 115 nm diameter soluble nanoplexes. For coating of the nanoplex surface with a lipid bilayer we introduced a hydrophobic tether, stearyl-octa-arginine (SR8). The indicated peptides were dissolved in methanol and combined with lipid mixtures in chloroform, followed by drying at RT under a nitrogen flow. The dry residues were hydrated with nanoplexes in Hepes, pH 7.4 yielding after a 30 min incubation at RT, rather monodisperse nanoparticles having an average diameter of 150–300 nm, measured by DLS and cryo-TEM. Studies with cell cultures showed the above peptides to yield expression levels comparable to those obtained using Lipofectamine 2000. However, unlike the polydisperse aggregates formed upon mixing Lipofectamine 2000 and plasmid, the procedure described yields soluble, and reasonably monodisperse nanoparticles, which can be expected to be suitable for gene delivery in vivo, using intravenous injection.

1. Introduction

In order to provide a real therapeutic utility, gene therapy requires an efficient uptake and insertion of genes into individual cells [1]. Because of the cytotoxicity and immunogenicity occasionally associated with viral gene delivery, non-viral vectors continue to be actively developed. Two currently studied non-viral approaches are i) polyplexes, i.e. complexes of plasmids and polymers, and ii) lipoplexes, composed of plasmids and cationic lipids [2,3]. However, the transfection levels achieved so far have been inferior to those obtained using viruses. Endocytosis is believed to represent the major cellular route for the uptake of these vectors [4,5], however, after internalization the majority of plasmids in the above complexes remain within endocytic vesicles [5–7]. Accordingly, there is a need to develop means to avoid the entrapment and degradation of plasmids in this compartment [6]. For this utility additives such as membrane disruptive pH-sensitive peptides, fusogenic lipids, lysosomotropic agents, 'synthetic' viruses, toxins, and different polymers have been incorporated into gene delivery systems [2,6,8–17]. Among these, peptides are gaining increasing attention because of the ease of their synthesis and introduction into different gene delivery systems [9,18,19]. Moreover, peptides are biodegradable, of small size, low cytotoxicity and immunogenicity, yet able to promote the escape of plasmids from endosomes, similarly to viruses [9,19–23]. Features such as DNA condensation, membrane translocation together with cellular and nuclear targeting further emphasize the potential use of peptides in gene delivery systems [9,17,20].

Several approaches have been used to optimize the amino acid sequences of cell penetrating peptides to enhance gene delivery by

Abbreviations: aBom, acidic bombolitin V; aLL-37, acidic LL-37; aMel, acidic melittin; AMP, antimicrobial peptides; caAM, calcein acetoxymethylester; Chol, cholesterol; cnDNA, condensed DNA; cryo-TEM, cryo-transmission electron microscopy; DAPI, 4′, 6-diamidino-2-phenylindole; DIC, differential interference contrast; DLS, dynamic light scattering; DMEM, Dulbecco's modified Eagle's medium; DOPE, 1,2-dioleoyl-*sn*-glycero-3-phosphoethanolamine; eggPC, egg phosphatidylcholine; emGFP, emerald green fluorescent protein; emGFP-Math1, emerald green fluorescent protein and *Math1* gene construct; EtBr, ethidium bromide; FCS, fetal calf serum; Glu, glutamic acid; HPLC, high-performance liquid chromatography; hRBC, human red blood cells; MTT, (4,5-dimethylthiazol-2-yl)2,5-diphenyl-tetrazolium bromide; PBS, phosphate buffered saline; PDI, polydispersity index; pDNA, plasmid DNA; pSEP, pH sensitive endosomolytic peptides; SR8, stearyl-octa-arginine; Z_{av}, average hydrodynamic diameter

* Corresponding author at: Helsinki Biophysics and Biomembrane Group, Department of Biomedical Engineering and Computational Science, Aalto University, P.O. Box 12200 (Otakaari 3J), FI-00076, Espoo, Finland. Tel.: +358 505404600.
E-mail address: Paavo.Kinnunen@aalto.fi (P.K.J. Kinnunen).
[1] These authors contributed equally to this work.
[2] Current address: Laboratory of Radiochemistry, Department of Chemistry, University of Helsinki, Helsinki, Finland.

http://dx.doi.org/10.1016/j.bbamem.2014.11.008
0005-2736/

Table 1
Amino acid sequences of the wild type and modified AMP.

Peptides	Sequences
LL-37	L L G D F F R K S K E K I G K E F K R I V Q R I K D F L R N L V P R T E S
aLL-37	10 20 30 C L L G D F F **E E** S **E** E **E** I G **E** E F **E E** I V Q **E** I **E** D F L **E** N L V P **E** T E S 10 20 30
Melittin	G I G A V L K V L T T G L P A L I S W I K R K R Q Q
aMel	10 20 C G I G A V L **E** V L T T G L P A L I S W I **E E E E** Q Q 10 20
Bombolitin V	I N V L G I L G L L G K A L S H L
aBom	10 C I N V L G I L G L L G **E** A L S **E** L 10

Below each sequence is shown the modified sequence with the introduced substitutions by Glu underlined and bold.

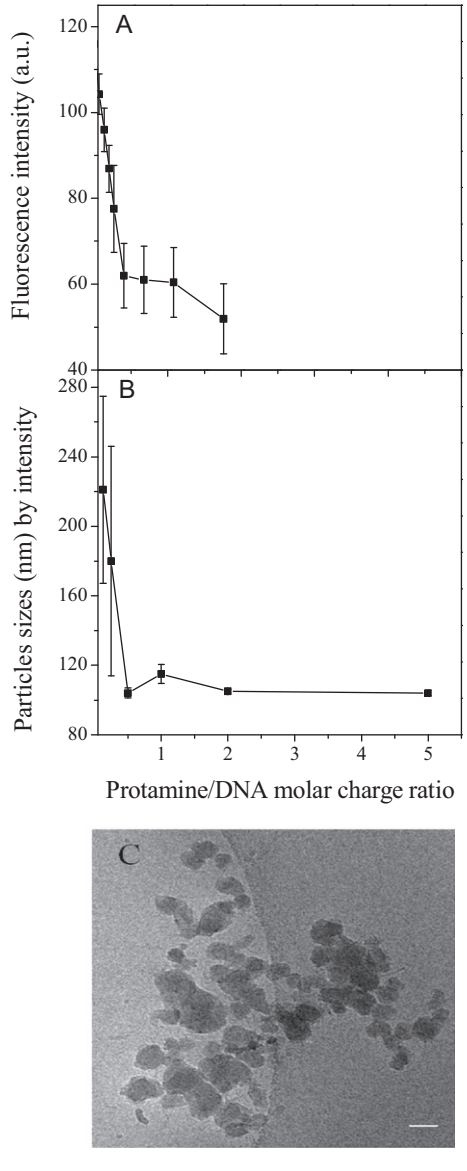

Fig. 1. Panel A: Condensation by protamine of the emGFP-Math1 plasmid monitored by the EtBr displacement assay. Panel B: Sizes of protamine–DNA complexes determined by DLS with increasing concentrations of protamine sulfate. Both panels depict mean and standard error for three independent experiments. Panel C: Cryo-TEM images of protamine–DNA complexes prepared at 1:1 charge ratio (7.4 μg protamine sulfate and 10 μg DNA) (15.15 nmol in base-pairs). Scale bar = 100 nm.

Table 2
Compositions of the nanoplexes given as molar ratios of the indicated peptides and lipids.

Nanoplexes	aLL-37	aMel	aBom	SR8	DOPE	eggPC	Chol
A				0.1	0.4	0.3	0.2
B	0.015			0.1	0.4	0.285	0.2
C	0.03		0.1	0.4	0.27	0.2	
D		0.03		0.1	0.4	0.27	0.2
E			0.03	0.1	0.4	0.27	0.2

facilitating endosomal escape [17,20,24–32]. pH-sensitive peptides were first developed and utilized, but their toxicity at physiological pH 7.4 is restricting their use [30]. A limited number of endosomolytic peptides have been described in the literature [6,9,24], mostly derived from viral proteins such as HA2, HA2-TAT, INF7, HGP, H5WYG, GALA, KALA, and E5WYG [6,8–12,15,18,23,25], in some cases resulting in a remarkable enhancement of gene expression. Peptides such as listeriolysin O, diphtheria toxin, exotoxin A, shiga toxin, cholera toxin, ricin, saporin, gelonin, and melittin were derived from bacteria, plants, and animals [6,8,13,26]. Also histidine-rich endosomolytic peptides and imadazole containing biopolymers have been made and characterized [20,27–29] for this purpose. However, principles for the design of endosomolytic peptides and their role in gene expression remain incompletely understood.

We here report the characterization of endosomolytic peptides derived from three membrane active antimicrobial peptides (AMP). To understand the molecular basis of their pH-sensitive cellular toxicity, we studied their hemolytic activity by the integrity of human red blood cells (hRBC) assessed by the release of hemoglobin and the calcein acetoxymethylester (caAM) assay. Transfection of 3T3 cells by condensed plasmid incorporating nanoparticles containing these peptides was studied and compared to transfection by the commercial reagent Lipofectamine 2000.

2. Materials and methods

2.1. Materials

Protamine sulfate and caAM were from Sigma. Stearoyl octaarginine (SR8) was from Storkbio (Tallin, Estonia). 1,2-Distearoyl-*sn*-glycero-3-phosphoethanolamine (DOPE), egg phosphatidylcholine (eggPC), and cholesterol (Chol), were from Avanti Polar Lipids (Alabaster, AL). The purity of lipids was checked by thin-layer chromatography on silicic acid coated plates (Merck, Darmstadt, Germany) developed with a chloroform/methanol/water mixture (65:25:4, v/v/v). Examination of the plates after iodine staining revealed no impurities. Lipid concentrations were determined gravimetrically with a high precision electrobalance [33]. The emGFP-math1 plasmid pcDNA6.2/C-EmGFP-Math1 [34] was used as a model for complex preparation and transfection experiments. Other chemicals were of analytical grade and from standard sources.

Table 3
Particle sizes and polydispersities by DLS for the plasmid DNA (pDNA) nanoparticles before and after the addition of indicated lipids and the peptides (Table 2). The content of the peptides is expressed in terms of mol% of the total amount of lipids and SR8.

Nanoplexes (See Table 2)	Peptide added (mol%)	Z_{av} diameter	PDI
A	None, control	194 ± 42.65	0.37 ± 0.12
B	aLL-37 (1.5 mol%)	198 ± 10.25	0.39 ± 0.04
C	aLL-37 (3 mol%)	927.47 ± 191.9	0.82 ± 0.14
D	aMel (3 mol%)	179.9 ± 17.46	0.27 ± 0.003
E	aBom (3 mol%)	186.23 ± 42.98	0.4 ± 0.16

2.2. Peptide synthesis, fluorescent labeling and purification

Peptides [Table 1] were purchased from Caslo, Denmark and were synthesized using standard Fmoc chemistry and purified by high-performance liquid chromatography (HPLC) to >97% purity, with sequences confirmed by mass spectrometry. When indicated these peptides were labeled at their N-terminal cysteine [35]. In brief, the indicated pH sensitive endosomolytic peptides (pSEP) and rhodamine-maleimide were incubated at a 1:1.3 M ratio for 3 h in a mixture (1:1, by vol.) of 100 mM Hepes, pH 7.0 and methanol at RT with constant stirring. The resulting conjugates were purified by HPLC on a C18 reverse phase column (Amersham Biosciences, Uppsala, Sweden) eluted with a linear gradient from 20 to 80% acetonitrile in water with 0.1% trifluoroacetic acid at a flow rate of 1 mL/min. Samples were monitored for absorbance at 540 nm. Fractions corresponding to the peptide–rhodamine conjugates were collected and lyophilized.

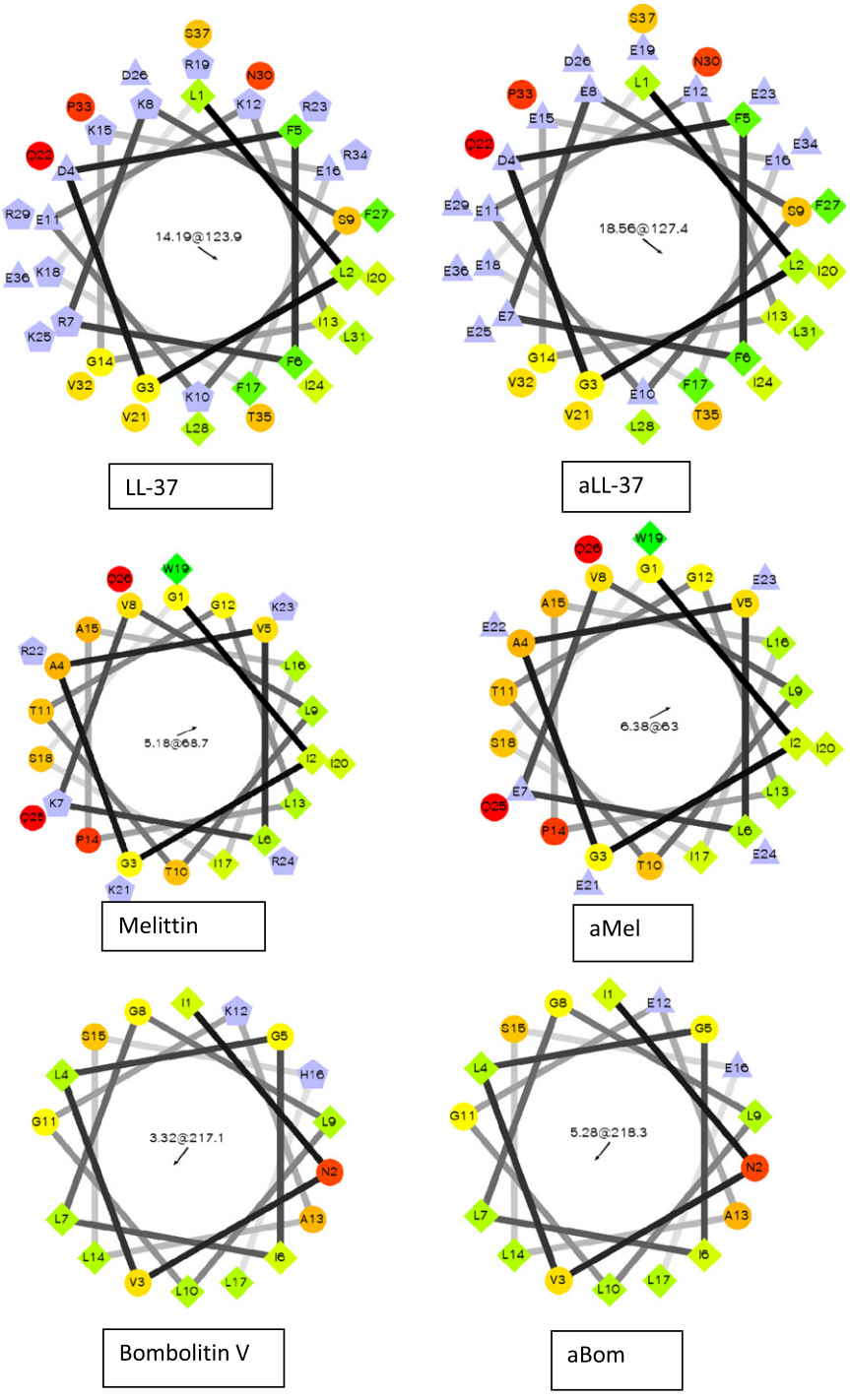

Fig. 2. Helical wheel diagrams of AMP and their analogs. The helical wheel projection figures are snaphots of Java Applet by Armstrong and Zidovetzki (University of California at Riverside, CA at http://rzlab.ucr.edu/scripts/wheel/wheel.cgi). The most hydrophobic residue is green with the intensity of color decreasing proportionally to the hydrophobicity, with zero hydrophobicity coded by yellow. Hydrophilic residues are coded by red with darker red corresponding to more hydrophilic (uncharged) residues, with the intensity of red decreasing proportionally to the hydrophilicity. For the sake of clarity and easier comparison with the wt peptides the N-terminal Cys has been omitted from the sequences of the analogs.

2.3. Binding to hRBC

The binding of the rhodamine-labeled pSEP to hRBC at pH 5.0 (150 mM NaCl, 15 mM citric acid) and 7.4 (150 mM NaCl, 20 mM Hepes) was assessed by fluorescence microscopy (Zeiss LSM-510 META microscope with a 63×, 1.4 NA Plan apochromate (oil immersion) objective). hRBC were plated on poly-L-Lys-coated slides and incubated with the indicated rhodamine-labeled pSEP for 30 min in either pH 5.0 or pH 7.4 [36,37], and subsequently fixed with 2% paraformaldehyde for 15 min and washed extensively with phosphate buffered saline (PBS). For confocal scanning, slides were mounted in 80% glycerol.

2.4. Assay for hRBC cell membrane integrity

CaAM is non-fluorescent and cell permeable and in live cells becomes hydrolyzed by intracellular esterases yielding a strongly fluorescent calcein anion, which is retained in the cytoplasm [38]. Accordingly, release of caAM can be used to assess e.g. peptide induced cell membrane permeabilization. For this purpose hRBC (0.6%, v/v in the indicated buffer) were incubated with 8 μM caAM in PBS for 1 h, whereafter free caAM and calcein were removed by washing the cells several times with PBS [38]. hRBC were then resuspended in either 150 mM NaCl, 20 mM Hepes, pH 7.4, or 150 mM NaCl, 15 mM citric acid, pH 5.0. The indicated peptides were subsequently added (5, 10, and 15 μM), followed by a 30 min incubation at 37 °C. Fluorescence intensities for calcein were measured with a Perkin Elmer spectrofluorometer in the timedrive mode using excitation and emission wavelengths of 490 and 515 nm, respectively [36]. The percentage of calcein release was calculated from:

$$\%\ \text{Calcein release} = \left[F_p - F_c / F_t - F_c\right] \times 100$$

where,

F_p fluorescence of sample containing peptide,
F_c fluorescence of sample without peptide, and
F_t fluorescence of sample after the addition of Triton X-100 (0.01% final concentration).

2.5. Assay for hemolysis

Fresh hRBC from healthy volunteers were isolated from the blood collected in the presence of an anticoagulant (heparin) and washed 3–4 times with PBS [10,30,36]. hRBC were suspended at 6% (v/v) in either pH 7.4, or pH 5.0 buffers in a final volume of 200 μL. pSEP dissolved in either pH 7.4, or 5.0 buffers as above, were then added. Subsequently, after a 30 min incubation at 37 °C samples were centrifuged for 10 min at 2000 rpm, and the release of hemoglobin into the supernatant was monitored by measuring the supernatant absorbance at 535 nm in a 96-well microplate reader (SpectraFluor plus, Tecan Gmbh, Salzburg, Austria) equipped with a 535 nm filter (10 nm bandpass). For negative and positive controls, hRBC in PBS (A_{blank}) and in 0.2% (v/v, final concentration) Triton X-100 (A_{triton}) were used, respectively. The percentage of hemolysis was calculated as described [36] from:

$$\%\ \text{hemolysis} = \left[\left(A_{sample} - A_{blank}\right) / \left(A_{triton} - A_{blank}\right)\right] \times 100.$$

2.6. Plasmid condensation and assembly of nanoplexes

Complexes of the 6093 base-pair emGFP-Math1 plasmid and protamine sulfate were prepared as described by El-Sayed et al. [23]. Accordingly, 10 μg (corresponding to 15.15 nmol in base-pairs) of the above plasmid was first condensed in 250 μl Hepes buffer, pH 7.4 by adding 7.4 μg (1.45 nmol) of protamine sulfate to yield a phosphate to nitrogen ratio of 1:1. Condensation of DNA was monitored by the ethidium bromide (EtBr) displacement assay [24]. DNA (10 μg) and EtBr (1 μg) were first complexed in a cuvette in 2 mL of 10 mM Hepes buffer, pH 7.4. Increasing concentrations of protamine sulfate were then added into this mixture and fluorescence intensity recorded using a spectrofluorometer (Varian eclipse) with excitation and emission wavelengths of 510 and 595 nm, respectively with the observed decrease in fluorescence reflecting the dissociation of EtBr from the plasmid (Fig. 1) upon its condensation due to the binding of protamine sulfate. The solution with the condensed plasmid (0.06 mM base-pairs) was characterized by dynamic light scattering (DLS, Zetasizer Nano ZS, Malvern Instruments Ltd., UK) yielding an apparent hydrodynamic particle diameter (Z_{av}) of 115 nm. Lipids (DOPE, eggPC, and Chol) were dissolved in chloroform, while SR8 and the indicated peptides were in methanol. The specified mixtures (Table 2) were mixed in the above organic solvents and the latter then evaporated using a gentle stream of nitrogen, whereafter the dry peptide/lipid residues were maintained under reduced pressure overnight to remove traces of solvents. Subsequently, 250 μl of the above nanoplex solution (10 μg plasmid) was added to hydrate the dry peptide/lipid film (75.5 μg total lipid) for 30 min at RT, followed by a 1 min incubation at RT in a bath type sonicator. The Z_{av} and polydispersity indexes (PDI) of the complexes forming after the addition of the indicated pSEP and lipids (Table 3) were determined at 25 °C by DLS.

Table 4
Comparison of the wild type and modified sequences for the presence of aggregating and amyloid forming sequences predicted by AGGRESCAN and PASTA algorithms.

Peptide	AGGRESCAN		PASTA	
	a	b	c	d
LL-37	–	−14.4	13–30	−4.25ap
aLL-37	1–5	−20.8	28–33	−3.30p
Melittin	3–13, 15–20	16.0	16–20	−5.03p
aMel	3–14, 16–20	10.4	17–21	−5.03p
Bombolitin V	1–12	41.0	1–7	−6.08p
aBom	1–13	37.2	2–8	−6.08p

a. Aggregation-prone segments (hot spots) predicted by AGGRESCAN.
b. Aggregation score by AGGRESCAN
c. Amyloidogenic regions predicted by PASTA.
d. Free energy calculated by PASTA and relative orientation of neighboring β-strands in the fibril core, p = parallel, ap = antiparallel.

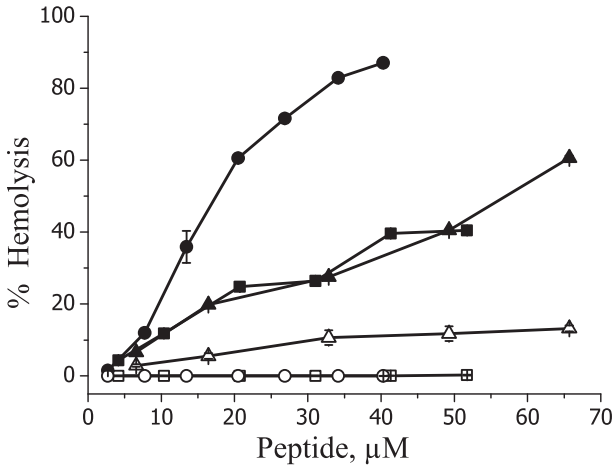

Fig. 3. Hemolysis of hRBC by aLL-37 (○, ●), aMel (□, ■), and aBom (Δ, ▲) at pH 7.4 (open symbols) and at pH 5.0 (filled symbols). Each point represents the mean of three independent experiments with error bars indicating standard deviations.

2.7. Transfection of 3T3 cells

NIH 3T3 cells (ATCC, Boras, Sweden) were cultured in Dulbecco's modified Eagle's medium (DMEM, Sigma, St Louis, MO, USA) supplemented with 10% fetal calf serum (FCS) (Invitrogen, USA) and 4 mM L-glutamine (Sigma Aldrich, USA). One day prior to their transfection, the cells were trypsinized and replated in 4-well chamber slides (Lab-Tek®II, Nalge Nunc International, Naperville, USA) at 1.5×10^5 cells per well in 1 mL of fresh FCS-glutamine-DMEM medium. Nanoplexes were then added to the cells (7.9 μg DNA in 1 mL DMEM) and incubated for 5 h, whereafter the transfection medium was replaced with fresh complete medium and the cells were incubated for another 36 h. Control cells were transfected using the same amount of the plasmid together with the commercial transfection reagent Lipofectamine 2000 (Invitrogen, USA), according to the manufacturer's instructions. After 36 h post-transfection, the cells were washed three times for 1 min with PBS and fixed with 4% paraformaldehyde for 30 min. Nuclei were counterstained with 4′, 6-diamidino-2-phenylindole (DAPI, 10 ng/mL, Sigma-Aldrich, USA) for 10 min and the cells were then mounted with Fluoromount (Sigma, USA) for confocal fluorescence microscopy [34] using a Olympus IX70 microscope with ANDOR IQ camera and an Ar–Kr laser for excitation at 488 and 568 nm. emGFP emission was recorded using a 525/50 filter. DAPI was excited using a 340–380 nm filter and detected using a 500 nm long-pass filter. Cells expressing emGFP were counted as positive using Image J (http://rsb.info.nih.gov/nih-image) and cells with DAPI counterstained nuclei were defined as total number of cells (10^4 cells were counted). Transfection efficiencies were calculated as the percentage of emGFP positive cells from the total number of cells.

2.8. Assay for cell viability

Viability of NIH 3T3 cells was determined to check for possible toxicity of the nanoplexes [13,23,30,37]. Accordingly, 10^4 cells per well were plated in 96-well plates, followed by an overnight incubation in a CO_2 incubator for adherence. The complete media were discarded from the plate, and 200 μl incomplete media per well were added. Concentration of nanoplexes on the basis of their content of DNA was 0.012 mM (1.58 μg DNA in 200 μl). After a 5 h incubation the transfection media was replaced with fresh complete medium and the cells were incubated for another 36 h under the same conditions. 20 μL of MTT (3-(4,5-dimethylthiazol-2-yl)-2,5-diphenyltetrazolium bromide, 5 mg/mL in PBS) was added to each well. After incubation for 3 h, media were discarded from the 96-well plates, and 200 μl of dimethyl sulfoxide (DMSO) was added to each well to dissolve the MTT crystals. The viability of cells in culture medium without additions was taken as 100%. The plates were measured for absorbance at 550 nm using a microplate reader.

3. Results

3.1. Design of AMP-derived endosomolytic peptides

Many viruses expose on their surface proteins enriched in acidic amino acids. Such sequences could be potentially sensitive to pH and involved in the pH-dependent disruption of endosomal membranes so as to release the viral genome into the cytoplasm of the target cells, thus enabling escape from the endosomes [6,8–10,23,30,32,39,40]. Several peptides derived from viral proteins have been shown to have

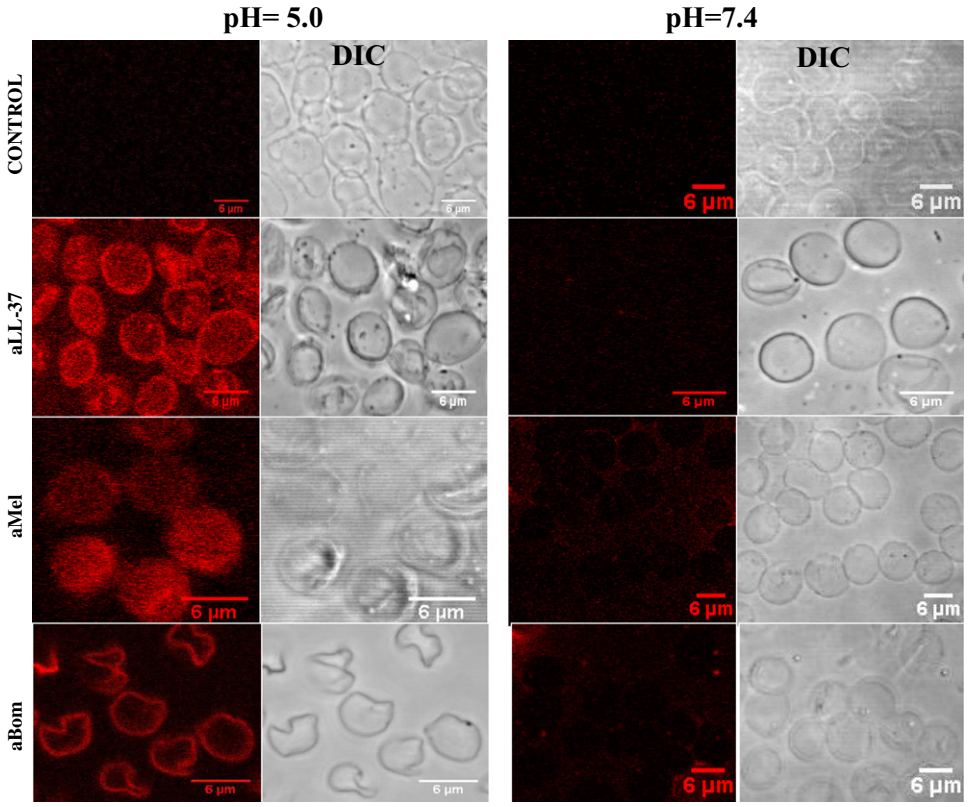

Fig. 4. Comparison of the binding of rhodamine-labeled pSEP to hRBC at pH 5.0 and pH 7.4 imaged by confocal microscopy. Rhodamine-labeled peptides, aLL-37, aMel, and aBom were added to hRBC whereafter both fluorescence and differential interference contrast (DIC) images were recorded. hRBC were plated on poly-L-lysine coated slides and incubated with the indicated peptides (~7.0 μM) for 30 min at pH 5.0 (150 mM NaCl, 15 mM citric acid) or 7.4 (150 mM NaCl, 20 mM Hepes). Subsequently, cells were fixed in 2% paraformaldehyde (10 min) and washed extensively with PBS. For confocal imaging slides were mounted in 80% glycerol.

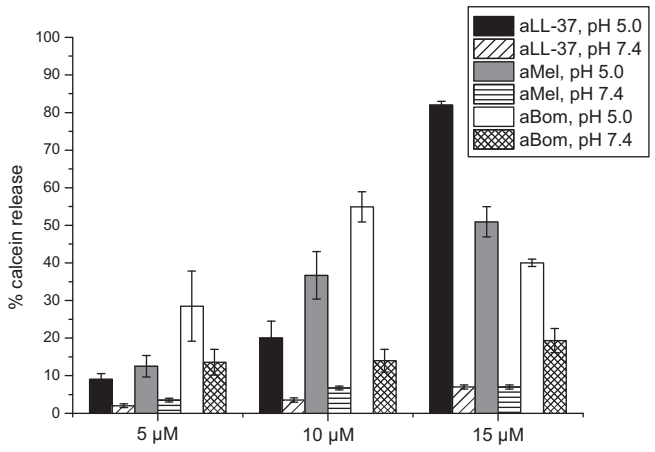

Fig. 5. Comparison of calcein release by the three AMP-analogs (each at 5, 10, and 15 μM concentration), assessed for 8 μM calcein-AM entrapped in hRBC at pH 5.0 (150 mM NaCl, 15 mM citric acid, filled columns) and 7.4 (150 mM NaCl, 20 mM Hepes, hatched columns, mean and standard error for 3 different experiments performed in triplicates). Calcein release was significant at pH 5.0 for both aLL-37 and aMel. However, aBom showed less pronounced difference in calcein release at pH 5.0 and 7.4. This could relate to aBom having at pH 7.0 the smallest net negative charge (−2) due to Glu, in comparison to aMel (−5) and aLL-37 (-16).

pH dependent cytotoxic activity. The sequences of these peptides are enriched in glutamic acid (Glu), which could relate to their toxicity at acidic pH. For example, INF7 is a glutamic acid rich peptide, which shows significant toxicity at pH 5.0, yet negligible toxicity in a similar concentration at pH 7.0 [23]. Likewise, GALA, which is enriched in acidic amino acids, shows significant and negligible toxic activity at pH 5.0 and 7.0, respectively [11]. Glu is partially protonated at pH 5.0 and this appears to be sufficient to make these peptides responsive to pH (10, 11, 30, 40). The above considerations led us to design pH sensitive peptides from naturally occurring membrane-permeabilizing antimicrobial peptides. We hypothesized that it could be possible to obtain pH sensitive endosomolytic peptides from membrane disrupting AMP by replacing their basic amino acids by Glu. More specifically, we chose three well studied AMP, viz. LL-37, melittin, and bombolitin V, and modified these by substituting all basic amino acids for Glu, followed by the testing of their pH sensitivity and toxicity. Cysteine was added at their N terminus to allow for coupling of rhodamine maleimide. For these peptides, both their amphipathic character as well as hydrophobicities remain comparable to the parent peptides (Fig. 2), and all three analogs reveal amphipathic helices, both when partially protonated (pH 5.0) and deprotonated (pH 7.0). Furthermore, their propensity for aggregation and amyloid formation was analyzed by AGGRESCAN [41] and PASTA [42] algorithms (Table 4) with only a slight reduction evident in the respective scores, when comparing the acidic peptides with the native, wild type AMPs. Unfortunately, while it would be of interest to see the impact of the protonation of Glu on the AGGRESCAN and PASTA scores, these algorithms do not allow varying pH.

The positive charges of AMPs are currently believed to be needed to target them to acidic phospholipids on the outer surface of microbial membranes. However, this property is not needed for transfection. The net negative charge of the modified peptides would at neutral pH cause electrostatic repulsion so as to maintain these peptides in a non-aggregated state while bound to membrane because of their amphipathic moment, which is retained after the substitution of Glu for basic residues (Fig. 2). Yet, in keeping with the tendency of these peptides for self-association, abrogating a fraction of the negative charges upon protonation of Glu at pH 5.0, abolishes the Coulombic repulsion, allowing subsequent peptide aggregation and permeabilization of the adjacent endosomal membrane somewhat analogously to the neutralization of the positive charges of AMPs upon complex formation with acidic phospholipids [43].

The possibilities for varying the sequences even in these small peptides are prohibitively large. Therefore, we chose to limit the present study to the above substitution by Glu and refrained from introducing other changes. Moreover, the aim of this study was to characterize the designed peptide analogs, so more rigorous testing was limited to these.

3.2. Characterization of the endosomolytic peptides

Melittin possesses notoriously high cytotoxic activity at both pH 7.4 and 5.0 [10]. LL-37 is a human antimicrobial peptide which shows negligible mammalian cell toxicity [44], while bombolitin V exhibits significant toxic activity against mammalian cells [45]. The dose dependent toxic activities of the designed analogs were tested at pH 7.4 and 5.0 by the hemolytic assay. The results were further augmented by comparing the localization by confocal microscopy of Rho-labeled peptides on hRBCs at pH 5.0 and 7.4 and calcein release at pH 7.4 and 5.0, so as to support the hemolysis data.

To study the impact of the replacement by Glu on the toxicity of these AMP and to see if this was sufficient to make these AMPs pH-sensitive, the hemolytic activities of the above AMP analogs were assessed at pH 5 and 7.4 using hRBC [30]. Acidic LL-37 (aLL-37) showed the highest lytic activity at pH 5 and induced at 20 μM concentration 60% cell lysis (Fig. 3). Acidic melittin (aMel) and acidic bombolitin V (aBom) were slightly less hemolytic than aLL-37 and induced only 20% lysis at 20 μM concentration and at pH 5.0. Notably, at pH 7.4 the hemolytic activities of the three peptides were very low (Fig. 3).

Binding of the rhodamine-labeled pSEP to hRBC was compared at pH 5.0 and 7.4 by confocal fluorescence microscopy. Fluorescence of the labeled pSEP was seen on the surface of hRBC at pH 5.0, in keeping with the association of pSEP to the cells (Fig. 4). However, at pH 7.4, the apparent binding of all three fluorescent pSEP onto hRBC was very weak (Fig. 4). In this context it is worth emphasizing that the fluorescence of rhodamine will be enhanced in a non-polar environment, such as upon entering the membrane hydrocarbon (acyl chain) region,

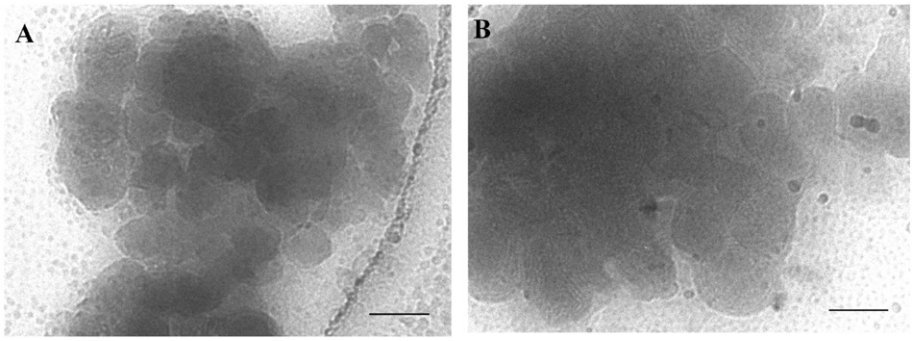

Fig. 6. Cryo-TEM images of nanoplexes, with (Panel A) aMel and (Panel B) aBom. Scale bar = 100 nm.

where they are expected to be accommodated upon their aggregation in hRBC membranes at pH 5.0, causing permeabilization. Accordingly, the recorded fluorescence intensities should not be taken as a direct measure of the amount of peptide bound at pH 5.0 and 7.4.

To assess membrane permeabilization by these three pSEP, release of entrapped calcein from hRBC was measured at pH 7.4 and 5.0. aLL-37 (~15 μM) induced a ~82% release of calcein at pH 5.0 (Fig. 5), while ~15 μM aMel and aBom caused at pH 5.0–48% and ~35% calcein release, respectively. On the other hand, at pH 7.4 all three pSEP induced very low (~6–7 % for aLL-37 and aMel, and ~19% for aBom) calcein release (Fig. 5). Dose dependence of calcein release was also assessed at 5 and 10 μM peptide concentration (Fig. 5). The above data comply with hemolysis induced by these pSEP at pH 5.0, and a lack of hemolytic activity at pH 7.4 (Fig. 3).

3.3. Assembly and characterization of nanoplexes

Protamine sulfate has a high content of arginine and efficiently condenses DNA already at low concentrations [46,47], as demonstrated here by the ethidium bromide displacement assay [24], in keeping with a high affinity binding of protamine to DNA (Fig. 1). Upon approaching charge neutralization at a ~1:1 nitrogen to phosphate molar

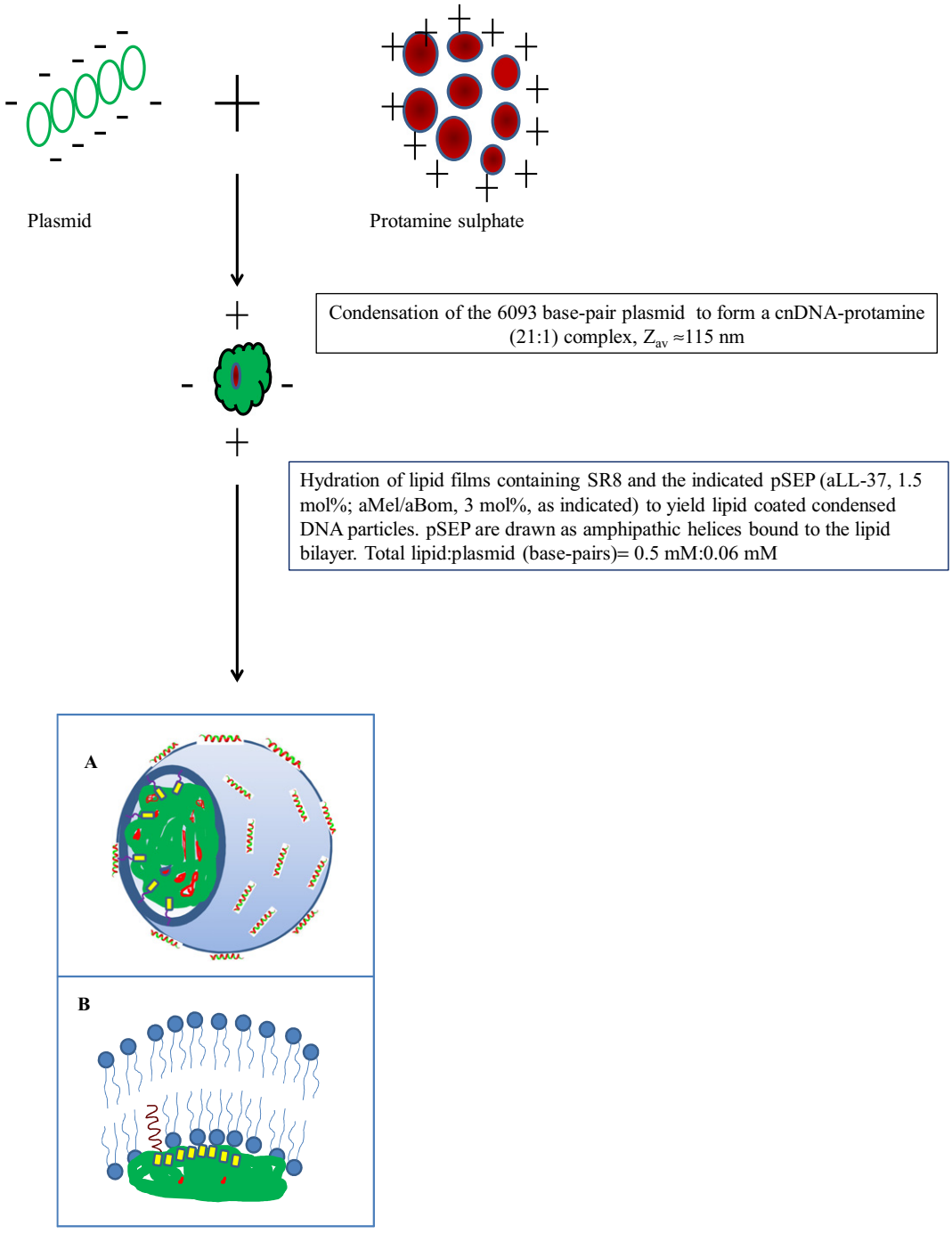

Fig. 7. Schematic illustration of the formation of cnDNA–protamine complexes and the subsequent addition of lipids, SR8 and pSEP to yield lipid coated nanoplexes. See text for details. The sizes of the molecules are not drawn to scale. Panel A: Schematic illustration of the lipid bilayer coated nanoplex, also depicting the anchoring of the bilayer to the stearoyl chains of SR8. Panel B: Magnified view of the tentative orientation of SR8 attached electrostatically to the DNA exposed on the surface of the nanoplex, with the stearoyl chain extending outward and attaching the lipid bilayer to the surface of the nanoplex.

ratio (for protamine/DNA), the average particle sizes were around ~115 nm with PDI of ~0.127, as characterized by DLS, and confirmed by cryo-transmission electron microscopy (cryo-TEM) (Figs. 1 and 6). Protamine has been suggested to contain a nuclear localization signal like amino acid sequence, which could promote the transfer of the plasmid from cytosol to nucleus [46].

For attaching pSEP to the protamine–DNA complexes the latter were first coated with a lipid bilayer [23]. To enhance the coating of the condensed DNA (cnDNA)–protamine complex by a lipid bilayer SR8 was employed to provide a hydrophobic alkyl chain tether on the surface of the nanoplexes (Fig. 7). SR8 can be expected to compete with protamine for the negatively charged plasmid on the surface of the nanoplexes, with its stearyl chain extending from the surface and representing a hydrophobic anchor for promoting the attachment of a lipid bilayer (Fig. 7, panel B). The lipid bilayer was necessary in order to attach the amphipathic pSEP noncovalently to the particle surface and to eventually protect the plasmid from nucleases. The indicated pSEP were included in the lipid films as described and are expected, because of their amphipathic character to bind to the lipid bilayer assembling onto the surface of the above nanoplexes. aMel or aBom (3 mol% with respect to total lipid) was included into the nanoplexes. However, this content of aLL-37 induced particle aggregation. Accordingly, only 1.5 mol% of aLL-37 was used (Table 3). Compositions of the nanoplexes are summarized in Table 2. The nanoplexes containing the above peptides had average sizes between 150 and 300 nm, as determined by DLS and cryo-TEM (Fig. 6). The nanoplexes were stable after one week at 4 °C from their preparation with DLS revealing no changes in Z_{av}.

3.4. Enhancement of transfection by pSEP

The expression of the plasmid contained in the lipid coated nanoplexes with and without pSEP was measured using 3T3 cells. Nanoplexes without pSEP transfected only ~1.8% of the cells while the commercial reagent Lipofectamine 2000 transfected ~11.9%. Inclusion of pSEP into nanoplexes increased emGFP expression significantly, with aLL-37, aMel, or aBom containing nanoplexes yielding transfection levels of ~9.2, ~7.6 and ~10.8%, respectively (Figs. 8 and 9). Nanoplexes with a higher content of aLL-37 (3 mol%) had low transfection efficiency (data not shown) and large aggregates were seen by DLS.

The viability of 3T3 cells exposed to nanoplexes both without and with pSEP was examined using the MTT assay, demonstrating lack of effect on cell viability by the pSEP containing nanoplexes (Fig. 10). Lipofectamine was not included as control because of its well known lack of toxicity seen in routine use for the transfection of cultured cells. Moreover, the chemical composition of Lipofectamine is proprietary, which would not allow for a meaningful molecular level interpretation of the data.

4. Discussion

The preparation of monodisperse nanoparticles with uniform size, shape and composition has been intensively pursued because of potentially allowing administration by i.v. injection. The major advantage of soluble monodisperse nanoparticles is that they should be able to pass through capillaries without causing thrombus formation and obstructing blood circulation so as to cause tissue infarct. Along these lines these particles should also be accessible for adding proper targeting ligands to achieve more cell specific responses [48] Instead, polydisperse aggregates obtained using Lipofectamine are not suitable for i.v. injection. Yet, they work very well with cell cultures, as these aggregates sediment and concentrate on the surface of cultured cells yielding efficient uptake.

A growing body of evidence suggests that lipid based delivery vectors represent a promising approach to practical gene therapy because of low toxicity, biodegradability, high cellular uptake, and easy surface functionalization by both covalent and non-covalent strategies [2,3,34]. However, this approach has been limited by poor gene delivery into the cytosol because of insufficient endosomal escape [2,3,6]. The addition of endosomolytic peptides has been shown to potentially remedy the latter and enhance gene expression by promoting gene transfer into the cytosol [9,23,31,32]. In this study we describe the design of three pH-sensitive peptides (aLL-37, aMel, and aBom) (Table 1), obtained by replacing the positively charged amino acids in their sequences with Glu. Confocal fluorescence microscopy demonstrated that rhodamine-labeled pSEP bind to hRBC at endosomal pH 5.0, with negligible fluorescence at pH 7.4 (Fig. 4). Likewise, these pSEP have high lytic activity against hRBC at pH = 5.0, with insignificant lysis seen at pH 7.4 (Fig. 3). Calcein release showed that all three pSEP induced significant hRBC membrane disruption at pH 5.0 and had a negligible effect at 7.4, (Fig. 5). The above data demonstrate pH-sensitivity of the membrane interaction of these peptides, in agreement with previous studies which have shown peptides containing negatively charged amino acids to have endosomolytic activity at acidic pH [10,11,30]. Overall, our results demonstrate that these pSEP permeabilize the

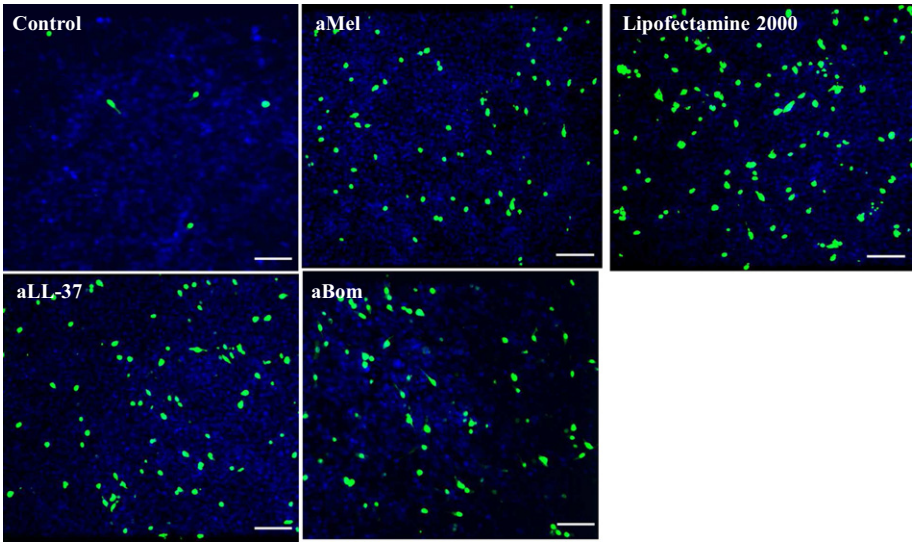

Fig. 8. Confocal fluorescence microscopy images of emGFP expression in 3T3 cells after the addition of pSEP containing nanoplexes with compositions compiled in Table 3, with aLL-37, aMel, and aBom as indicated. Cells transfected by nanoplexes without pSEP are shown as a control. For comparison transfection is illustrated with the same plasmid but using the commercial reagent Lipofectamine 2000. Scale bar = 100 μm.

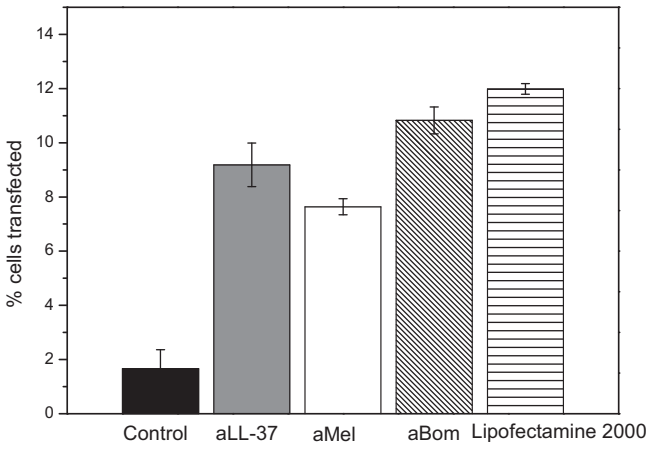

Fig. 9. Percentage of 3T3 cell transfected by the nanoplexes with the indicated pSEP, quantitated by emGFP fluorescence using image J software, illustrating mean and standard error for two different experiments. Control: Nanoplexes without pSEP, nanoplexes containing the indicated peptides aLL-37, aMel, and aBom. For comparison data is shown for cells transfected by the same plasmid and Lipofectamine 2000.

membrane selectively at pH 5.0, similarly to viruses which escape from endosomes at the moderately acidic pH of approx. 5.0 of the endosomes. [10,11,39,40].

Both Asp and Glu make peptides sensitive to pH [10,11,30] and several viruses contain surface proteins which are enriched in these residues. Both bear a net negative charge at pH of 7.4, and become partially protonated at pH = 5.0 [10,11,30,40]. Several endosomolytic agents have been designed to become protonated at endosomal pH of 5.0. [8,10,11,23,27–30,39,40] and are thus expected to destabilize the endosomal membrane, causing the escape of viruses from endosomes [10,11,39,40]. In a similar fashion, because of the membrane permeabilization of these AMPs these pSEP derived from AMP with Glu substituted for Lys and Arg should become membrane disrupting at endosomal pH. Protonation of Glu abrogates Coulombic repulsion between the membrane associated peptides and allows peptide aggregation, which has been concluded to be involved in membrane permeabilization [43].

Following endocytosis of the particles pSEP allows endosomal escape by breaking the endosomal membrane at acidic pH, resulting in the release of the nucleocapsid-like cnDNA protamine nanoparticles into the cytosol. The transfection efficiency of our nanoparticles was tested in 3T3 cells. Characterized by DLS (Table 3) and cryo-TEM (Fig. 6) the sizes of nanoplexes were 150–300 nm. The MTT assay for

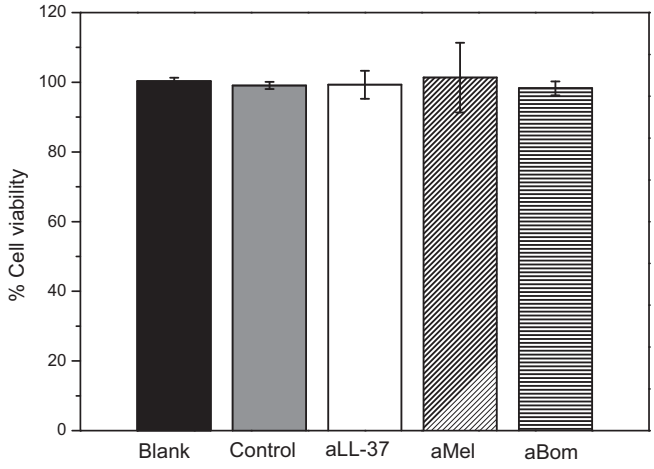

Fig. 10. Viability of 3T3 cells assessed by the MTT assay after the addition of nanoplexes containing the indicated peptides (means ± S.D. for five independent experiments). Blank: cell culture without nanoplexes, Control: nanoplexes without pSEP.

3T3 cells exposed to the nanoplexes both with or without pSEP, showed no loss of cell viability (Fig. 10).

The endocytic pathway is one of the main cellular uptake mechanism for most nanoparticles. Eventually, the material taken up by this mechanism becomes enclosed in a low pH environment of endosomes for degradation by the contained hydrolytic enzymes. We included into the nanoplexes peptides derived from AMP in order to augment gene expression by promoting gene delivery into the cytosol [Table 3]. Gene expression was visualized by confocal microscopy and quantified by analysis using image J. Our pSEP added to nanoplexes resulted in the transfection of 8–11% of cultured cells (Figs. 8, 9), at levels comparable to the transfection efficiency achieved using the commercial transfection reagent Lipofectamine 2000. Higher contents (3 mol%) of aLL-37 attenuated the expression of the reporter gene (data not shown), probably because of aggregation of nanoplexes [49] while both (3 mol%) aMel and aBom yielded significant transfection efficiencies corresponding to the levels observed using 1.5 mol% aLL-37.

Accumulating data suggest that pH-induced endosomal membrane destabilization as employed by viruses may be involved in the action of synthetic anionic peptides used to enhance gene delivery [6,9–11, 15,23,25,31,32,39,40]. This process is likely to underlie also the action of the endosomolytic peptides described here. These pSEP had appreciable membrane disruptive activity at pH 5.0 and are expected to utilize this property to promote the degradation of the endosomal membrane, thus promoting the entry of the nanoplexes into the cytoplasm. Our findings support the notion that modification of lipid nanoparticles with endosomolytic peptides by covalent or non-covalent strategy can be employed to obtain endosomal escape and elevated levels of gene expression. The non-viral pSEP modified lipid based nanocarriers described here are efficient, yet show no evidence for toxicity, presumably delivering the contained DNA into cells by a mechanism resembling that used by viruses.

It is relevant to keep the limitations of our strategy in mind, while making it clear that ample possibilities remain available for the design of novel functional peptides for improving gene transfer. Our present study should be considered just a small step towards establishing rational design principles for achieving more efficient peptides to augment transfection. Along these lines, our approach is simply focused on overcoming the endosomal trapping of DNA as a barrier for gene delivery. Much more work remains to be done to achieve synthetic virus-like particles conveying genes to specific cells in an efficient, safe manner.

Acknowledgments

This study was conducted in the European Community 6th framework program; contract NMP4-CT-2006-026556, NANOEAR, aimed at targeted drug & gene delivery into the cells of the inner ear.

References

[1] I.M. Verma, N. Somia, Gene therapy — promises, problems and prospects, Nature 389 (1997) 239–242.
[2] C. Tros de Ilarduya, Y. Sun, N. Duzgunes, Gene delivery by lipoplexes and polyplexes, Eur. J. Pharm. Sci. 40 (2010) 159–170.
[3] A. Elouahabi, J.M. Ruysschaert, Formation and intracellular trafficking of lipoplexes and polyplexes, Mol. Ther. 11 (2005) 336–347.
[4] A.F. Adler, K.W. Leong, Emerging links between surface nanotechnology and endocytosis: impact on nonviral gene delivery, Nano Today 5 (2010) 553–569.
[5] I.A. Khalil, K. Kogure, H. Akita, H. Harashima, Uptake pathways and subsequent intracellular trafficking in nonviral gene delivery, Pharmacol. Rev. 58 (2006) 32–45.
[6] A.K. Varkouhi, M. Scholte, G. Storm, H.J. Haisma, Endosomal escape pathways for delivery of biologicals, J. Control. Release 151 (2010) 220–228.
[7] H. Akita, R. Ito, I.A. Khalil, S. Futaki, H. Harashima, Quantitative three-dimensional analysis of the intracellular trafficking of plasmid DNA transfected by a nonviral gene delivery system using confocal laser scanning microscopy, Mol. Ther. 9 (2004) 443–451.
[8] E. Wagner, Application of membrane-active peptides for nonviral gene delivery, Adv. Drug Deliv. Rev. 38 (1999) 279–289.
[9] M.E. Martin, K.G. Rice, Peptide-guided gene delivery, AAPS J. 9 (2007) 18–29.

[10] C. Plank, B. Oberhauser, K. Mechtler, C. Koch, E. Wagner, The influence of endosome-disruptive peptides on gene transfer using synthetic virus-like gene transfer systems, J. Biol. Chem. 269 (1994) 12918–12924.
[11] W. Li, F. Nicol, F.C.J. Szoka, GALA: a designed synthetic pH-responsive amphipathic peptide with applications in drug and gene delivery, Adv. Drug Deliv. Rev. 56 (2004) 967–985.
[12] S.H. Min, D.C. Lee, M.J. Lim, H.S. Park, D.M. Kim, C.W. Cho, Y. Yoondo, Y.I. Yeom, A composite gene delivery system consisting of polyethylenimine and an amphipathic peptide KALA, J. Gene Med. 8 (2006) 1425–1434.
[13] M. Meyer, A. Zintchenko, M. Ogris, E. Wagner, A dimethylmaleic acid-melittin-polylysine conjugate with reduced toxicity, pH-triggered endosomolytic activity and enhanced gene transfer potential, J. Gene Med. 9 (2007) 797–805.
[14] G. Saito, G.L. Amidon, K.D. Lee, Enhanced cytosolic delivery of plasmid DNA by a sulfhydryl-activatable listeriolysin O/protamine conjugate utilizing cellular reducing potential, Gene Ther. 10 (2003) 72–83.
[15] A. Kichler, K. Mechtler, J.P. Behr, E. Wagner, Influence of membrane-active peptides on lipospermine/DNA complex mediated gene transfer, Bioconjug. Chem. 8 (1997) 213–221.
[16] K. Ciftci, R.J. Levy, Enhanced plasmid DNA transfection with lysosomotropic agents in cultured fibroblasts, Int. J. Pharm. 218 (2001) 81–92.
[17] A. Mann, G. Thakur, V. Shukla, M. Ganguli, Peptides in DNA delivery: current insights and future directions, Drug Discov. Today 13 (2008) 152–160.
[18] E.J. Kwon, S. Liong, S.H. Pun, A truncated HGP peptide sequence that retains endosomolytic activity and improves gene delivery efficiencies, Mol. Pharm. 7 (2010) 1260–1265.
[19] V.P. Torchilin, T.S. Levchenko, R. Rammohan, N. Volodina, B. Papahadjopoulos-Sternberg, G.G. D'Souza, Cell transfection *in vitro* and *in vivo* with nontoxic TAT peptide–liposome–DNA complexes, Proc. Natl. Acad. Sci. U. S. A. 100 (2003) 1972–1977.
[20] S.L. Lo, S. Wang, An endosomolytic Tat peptide produced by incorporation of histidine and cysteine residues as a nonviral vector for DNA transfection, Biomaterials 29 (2008) 2408–2414.
[21] I.A. Khalil, K. Kogure, S. Futaki, H. Harashima, Octaarginine-modified liposomes: enhanced cellular uptake and controlled intracellular trafficking, Int. J. Pharm. 354 (2008) 39–48.
[22] S. Boeckle, E. Wagner, M. Ogris, C- versus N-terminally linked melittin-polyethylenimine conjugates: the site of linkage strongly influences activity of DNA polyplexes, J. Gene Med. 7 (2005) 1335–1347.
[23] A. El-Sayed, T. Masuda, I. Khalil, H. Akita, H. Harashima, Enhanced gene expression by a novel stearylated INF7 peptide derivative through fusion independent endosomal escape, J. Control. Release 138 (2009) 160–167.
[24] S. Futaki, W. Ohashi, T. Suzuki, M. Niwa, S. Tanaka, K. Ueda, H. Harashima, Y. Sugiura, Stearylated arginine-rich peptides: a new class of transfection systems, Bioconjug. Chem. 12 (2001) 1005–1011.
[25] J.S. Wadia, R.V. Stan, S.F. Dowdy, Transducible TAT-HA fusogenic peptide enhances escape of TAT-fusion proteins after lipid raft macropinocytosis, Nat. Med. 10 (2004) 310–315.
[26] K. Sandvig, B. Spilsberg, S.U. Lauvrak, M.L. Torgersen, T.G. Iversen, B.V. Deurs, Pathways followed by protein toxins into cells, Int. J. Med. Microbiol. 293 (2004) 483–490.
[27] A. Kichler, C. Leborgne, J. Marz, O. Danos, B. Bechinger, Histidine-rich amphipathic peptide antibiotics promote efficient delivery of DNA into mammalian cells, Proc. Natl. Acad. Sci. U. S. A. 100 (2003) 1564–1568.
[28] A. Kichler, C. Leborgne, O. Danos, B. Bechinger, Characterization of the gene transfer process mediated by histidine-rich peptides, J. Mol. Med. 85 (2007) 191–201.
[29] D.W. Pack, D. Putnam, R. Langer, Design of imidazole-containing endosomolytic biopolymers for gene delivery, Biotechnol. Bioeng. 67 (2000) 217–223.
[30] S. Boeckle, J. Fahrmeir, W. Roedl, M. Ogris, E. Wagner, Melittin analogs with high lytic activity at endosomal pH enhance transfection with purified targeted PEI polyplexes, J. Control. Release 112 (2006) 240–248.
[31] H. Kamata, H. Yagisawa, S. Takahashi, H. Hirata, Amphiphilic peptides enhance the efficiency of liposome-mediated DNA transfection, Nucleic Acids Res. 22 (1994) 536–537.
[32] S. Simoes, V. Slepushkin, R. Gaspar, M.C. de Lima, N. Duzgunes, Gene delivery by negatively charged ternary complexes of DNA, cationic liposomes and transferrin or fusogenic peptides, Gene Ther. 5 (1998) 955–964.
[33] R. Tejera-Garcia, L. Connell, W.A. Shaw, P.K. Kinnunen, Gravimetric determination of phospholipid concentration, Chem. Phys. Lipids 165 (2012) 689–695.
[34] W. Zhang, Y. Zhang, R. Sood, S. Ranjan, E. Surovtseva, A. Ahmad, P.K. Kinnunen, I. Pyykko, J. Zou, Visualization of intracellular trafficking of Math1 protein in different cell types with a newly-constructed nonviral gene delivery plasmid, J. Gene Med. 13 (2011) 134–144.
[35] J. Zou, Y. Zhang, W. Zhang, S. Ranjan, R. Sood, A. Mikhailov, P.K. Kinnunen, I. Pyykko, Internalization of liposome nanoparticles functionalized withTrkB ligand in rat cochlear cell populations, Eur. J. Nanomed. 3 (2009) 8–14.
[36] A. Ahmad, S.P. Yadav, N. Asthana, K. Mitra, S.P. Srivastava, J.K. Ghosh, Utilization of an amphipathic leucine zipper sequence to design antibacterial peptides with simultaneous modulation of toxic activity against human red blood cells, J. Biol. Chem. 281 (2006) 22029–22038.
[37] A. Ahmad, S. Azmi, R.M. Srivastava, S. Srivastava, B.K. Pandey, R. Saxena, V.K. Bajpai, J.K. Ghosh, Design of nontoxic analogues of cathelicidin-derived bovine antimicrobial peptide BMAP-27: the role of leucine as well as phenylalanine zipper sequences in determining its toxicity, Biochemistry 48 (2009) 10905–10917.
[38] D. Bratosin, L. Mitrofan, C. Palii, J. Estaquier, J. Montreuil, Novel fluorescence assay using calcein-AM for the determination of human erythrocyte viability and aging, Cytom. A 66 (2005) 78–84.
[39] D. Mudhakir, H. Harashima, Learning from the viral journey: how to enter cells and how to overcome intracellular barriers to reach the nucleus, AAPS J. 11 (2009) 65–77.
[40] T. Wang, S. Yang, V.A. Petrenko, V.P. Torchilin, Cytoplasmic delivery of liposomes into MCF-7 breast cancer cells mediated by cell-specific phage fusion coat protein, Mol. Pharm. 7 (2010) 1149–1158.
[41] O. Conchillo-Sole, N.S. de Groot, F.X. Aviles, J. Vendrell, X. Daura, S. Ventura, AGGRESCAN: a server for the prediction and evaluation of "hot spots" of aggregation in polypeptides, BMC Bioinforma. 8 (2007) 65.
[42] A. Trovato, F. Seno, S.C. Tosatto, The PASTA server for protein aggregation prediction, Protein Eng. Des. Sel. 20 (2007) 521–523.
[43] A.K. Mahalka, P.K.J. Kinnunen, Binding of amphipathic α-helical antimicrobial peptides to lipid membranes: lessons from temporins B and L, Biochim. Biophys. Acta 1788 (2009) 1600–1609.
[44] S.M. Travis, N.N. Anderson, W.R. Forsyth, C. Espiritu, B.D. Conway, E.P. Greenberg, P.B. McCray Jr., R.I. Lehrer, M.J. Welsh, B.F. Tack, Bactericidal activity of mammalian cathelicidin-derived peptides, Infect. Immun. 68 (2000) 2748–2755.
[45] A. Argiolas, J.J. Pisano, Bombolitins, a new class of mast cell degranulating peptides from the venom of the bumblebee *Megabombus pennsylvanicus*, J. Biol. Chem. 260 (1985) 1437–1444.
[46] T. Masuda, H. Akita, H. Harashima, Evaluation of nuclear transfer and transcription of plasmid DNA condensed with protamine by microinjection: the use of a nuclear transfer score, FEBS Lett. 579 (2005) 2143–2148.
[47] S.N. He, Y.L. Li, J.J. Yan, W. Zhang, Y.Z. Du, H.Y. Yu, F.Q. Hu, H. Yuan, Ternary nanoparticles composed of cationic solid lipid nanoparticles, protamine, and DNA for gene delivery, Int. J. Nanomed. 8 (2013) 3033–3050.
[48] S. Ranjan, R. Sood, J. Dudas, R. Glueckert, A. Schrott-Fischer, S. Roy, I. Pyykkö, P.K.J. Kinnunen, Peptide-mediated targeting of liposomes to TrkB receptor expressing cells, Int. J. Nanomed. 7 (2012) 3475–3485.
[49] R. Sood, Y. Domanov, M. Pietiäinen, V.P. Kontinen, P.K.J. Kinnunen, Binding of LL-37 to model biomembranes: insight into target vs host cell recognition, Biochim. Biophys. Acta 778 (2008) 983–996.